

# Energy Redistribution Between Quasiparticles in Mesoscopic Silver Wires

F. Pierre, H. Pothier, D. Esteve, and M.H. Devoret

*Service de Physique de l'Etat Condensé, Commissariat à l'Energie Atomique,  
Saclay, F-91191 Gif-sur-Yvette, France*

*We have measured with a tunnel probe the energy distribution function of quasiparticles in silver diffusive wires connected to two large pads ("reservoirs"), between which a bias voltage was applied. From the dependence in energy and bias voltage of the distribution function we have inferred the energy exchange rate between quasiparticles. In contrast with previously obtained results on copper and gold wires, these data on silver wires can be well interpreted with the theory of diffusive conductors either solely, or associated with another mechanism, possibly the coupling to two-level systems.*

PACS numbers: 73.23.-b, 73.50.-h, 71.10.Ay, 72.70.+m.

The present understanding of metals at low temperature relies on Landau's theory of Fermi liquids. In this theory, the elementary excitations of the electron fluid are nearly independent fermionic quasiparticles.<sup>1</sup> The residual interactions depend on the efficiency of the screening of Coulomb interactions, and increase if electrons are scattered by impurities, surface or lattice defects.<sup>2,3</sup> These interactions can be probed through the shape of the energy distribution function in an out-of-equilibrium situation. We have found in previous experiments on copper<sup>4</sup> and gold<sup>5</sup> wires that the energy exchange rate between quasiparticles is stronger and has a different energy dependence than predicted by Altshuler and Aronov's (AA) theory of diffusive conductors.<sup>3</sup> In the present paper, we report measurements of distribution functions in silver wires, where the interactions appear to be in closer agreement with AA theory.

The experimental setup used to probe the energy exchange rate is shown in Fig. 1. A metallic diffusive wire of length  $L$  is connected at both ends

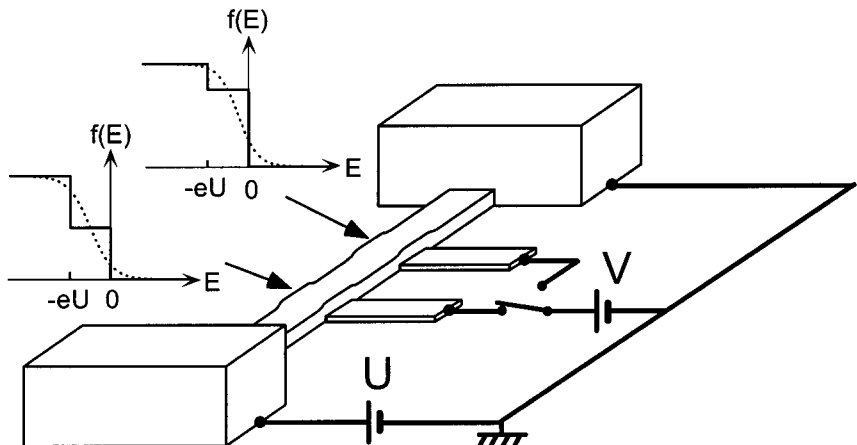


Fig. 1. Experimental layout: a metallic wire of length  $L$  is connected to large reservoir electrodes, biased at potentials 0 and  $U$ . In absence of interaction, the distribution function at a distance  $X = xL$  from the grounded electrode has an intermediate step  $f(E) = 1 - x$  for energies between  $-eU$  and 0 (solid curves) (we assume  $U > 0$ ). When interactions are strong enough to thermalize electrons, the distribution function is a Fermi function, with a space-dependent temperature and electrochemical potential (dotted curves). In the experiment, the distribution function is obtained from the differential conductance  $dI/dV(V)$  of the tunnel junction formed by the wire and a superconducting electrode placed underneath.

to large and thick electrodes called “reservoirs” in the following. The quasi-particle energy distribution  $f(x, E)$  at a distance  $X = xL$  from the right electrode, is obtained from the differential conductance  $dI/dV(V)$  of a tunnel junction between the wire and a superconducting electrode.<sup>4,6</sup> A voltage difference  $U$  is applied between the reservoirs in order to implement a stationary out-of-equilibrium situation. The shape of the distribution function  $f(x, E)$  depends on the average number of inelastic collisions a quasiparticle experiences during its diffusive motion from one of the electrodes to the position  $X$ , and on the amount of energy exchanged at each collision.

We present the results of four experiments, labeled A, B, C and D in the following. The wire length  $L = 5, 10$ , or  $20 \mu\text{m}$  is appended to the label; for instance the samples A5 and C20 are 5 and  $20 \mu\text{m}$ -long, respectively. All samples were fabricated by electron-gun evaporation of silver at several angles through a PMMA suspended mask patterned using e-beam lithography. The substrate was, as in our experiments on Cu and Au, thermally oxidized silicon. Samples with same labels (B5 and B10 on the one hand, D20a and

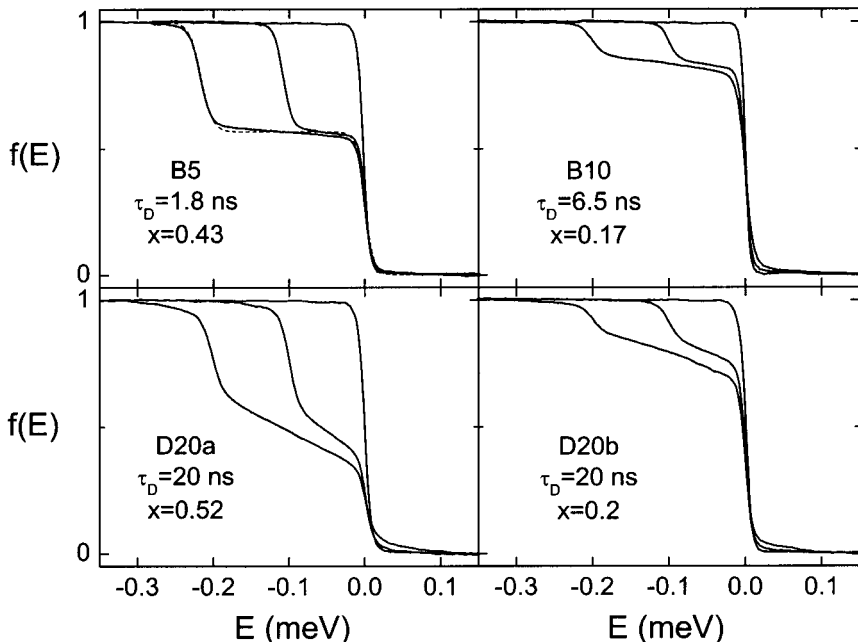


Fig. 2. Measured distribution functions for  $U = 0, 0.1$  and  $0.2$  mV in samples B5, B10, D20a and D20b (see Table 1). In the top left panel, the dotted line is the prediction for the non-interacting regime (Eq. (2)) for  $U = 0.2$  mV.

D20b on the other hand) were fabricated simultaneously. The thickness of the wires is 45 nm and their width  $w$  ranges between 65 nm and 150 nm. The electrodes at the ends of the wires are 400 nm-thick silver pads with an area of about  $1 \text{ mm}^2$ , thereby implementing adequate reservoirs.<sup>7</sup> The superconducting probes, made of aluminum,<sup>8</sup> were positioned at  $x = 0.5$  and/or at  $x = 0.2$ . The areas of the tunnel junctions are  $w \times 150$  nm and their tunnel resistances range between  $23 \text{ k}\Omega$  and  $130 \text{ k}\Omega$ . We estimated the diffusion coefficient  $D$  of quasiparticles, and hence the diffusion time  $\tau_D = L^2/D$ , from the low-temperature resistance of the wires. The samples were mounted in a copper box thermally anchored to the mixing chamber of a dilution refrigerator. Electrical connections were made through filtered coaxial lines,<sup>9</sup> and measurements were carried out at a temperature of 40 mK.

The distribution functions obtained at  $U = 0, 0.1$  and  $0.2$  mV are shown in Fig. 2. For  $U = 0$ ,  $f(E)$  is close to the expected Fermi function at the temperature of the refrigerator. For  $U \neq 0$ , the functions  $f(E)$  measured near the middle of the wire B5 (top left panel) display a sharp double step

with a plateau at height  $1 - x = 0.57$ . For comparison, we have plotted as a dotted line the best fit at  $U = 0.2$  mV with a linear combination of the Fermi functions of the reservoirs,<sup>10</sup> which is the expected distribution function in the non-interacting regime (see Refs.<sup>4,11</sup> and Eq. (2) below). The deviations from this regime are more apparent in sample D20a (bottom left panel), for which the diffusion time  $\tau_D = 20$  ns is significantly longer than in sample B5 where  $\tau_D = 1.8$  ns. In the right panels of Fig. 2 we show the distribution functions measured at the lateral position of samples B10 (top right panel) and D20b (bottom right panel). The height of the plateau well agrees with  $1 - x \approx 0.8$ , and the distribution functions are again more rounded for the wire with the longer diffusion time.

The distribution functions obtained in the experiments on copper and gold wires systematically display a scaling property:<sup>4</sup> as shown for a copper sample<sup>12</sup> in the right panel of Fig. 3,  $f(x, E)$  only depends, at each position, on the reduced variable  $E/eU$ . Such a scaling law is not observed in our silver samples: in particular, the slope of the plateau in the distribution functions of the wire D20a increases with  $U$  when plotted in reduced units (see the left panel of Fig. 3). This indicates that interactions between quasiparticles have a different energy dependence in the two types of samples. Interactions are also weaker in silver samples: as illustrated in Fig. 3, similar distribution functions are obtained for longer diffusion time in silver than in copper or gold samples.

In order to compare the energy distribution functions  $f(x, E)$  obtained experimentally with the theoretical predictions, we now explain how the energy exchange rate between quasiparticles determines  $f(x, E)$ . The stationary distribution function  $f(x, E)$  obeys the Boltzmann equation:<sup>11,13</sup>

$$\frac{1}{\tau_D} \frac{\partial^2 f(x, E)}{\partial x^2} + \mathcal{I}_{\text{coll}}(x, E, \{f\}) = 0 \quad (1)$$

where  $\mathcal{I}_{\text{coll}}(x, E, \{f\})$  is the collision integral due to interactions between quasiparticles. The boundary conditions are imposed by the reservoirs at both ends:  $f(0, E) = \left(1 + \exp \frac{E}{k_B T}\right)^{-1}$  and  $f(1, E) = \left(1 + \exp \frac{E+eU}{k_B T}\right)^{-1}$ .

In the absence of inelastic scattering  $\mathcal{I}_{\text{coll}} = 0$  and the distribution function  $f_0(x, E)$  is:<sup>11</sup>

$$f_0(x, E) = (1 - x)f(0, E) + xf(1, E). \quad (2)$$

The function  $f_0(x, E)$  has a well-defined plateau for  $|eU| \gg k_B T$ , as observed in sample B5 (see Fig. 2).

The collision term  $\mathcal{I}_{\text{coll}}(x, E, \{f\})$  is the difference of two terms: an in-collision term, the rate at which particles are scattered into a state of energy

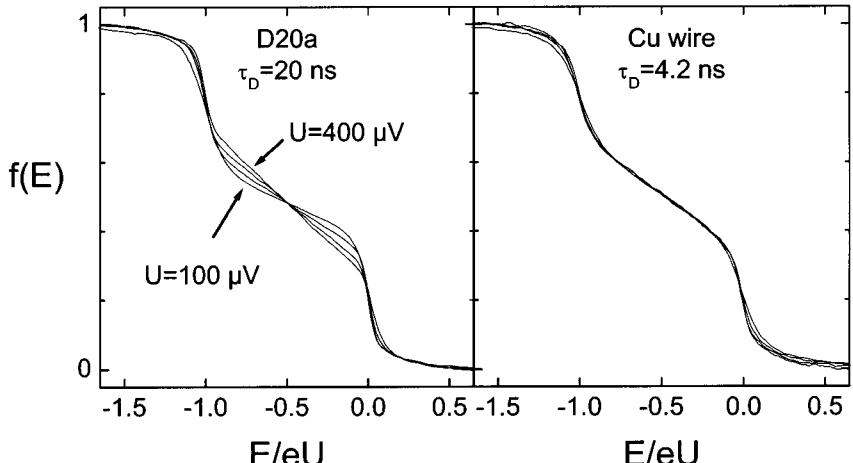


Fig. 3. Distribution functions for  $U = 0.1, 0.2, 0.3$ , and  $0.4 \text{ mV}$ , plotted as a function of the reduced energy  $E/eU$ . Left panel: Ag sample D20a; right panel: Cu sample,  $L = 5 \mu\text{m}$ .

$E$ , and an out-collision term:

$$\mathcal{I}_{\text{coll}}(x, E, \{f\}) = \mathcal{I}_{\text{coll}}^{\text{in}}(x, E, \{f\}) - \mathcal{I}_{\text{coll}}^{\text{out}}(x, E, \{f\}) \quad (3)$$

with

$$\begin{aligned} \mathcal{I}_{\text{coll}}^{\text{in,out}}(x, E, \{f\}) &= \int d\varepsilon dE' K(\varepsilon) \\ &\times f_{E+\varepsilon, E}^x (1 - f_{E, E-\varepsilon}^x) f_{E'}^x (1 - f_{E'+\varepsilon}^x) \end{aligned} \quad (4)$$

where the shorthand  $f_E^x$  stands for  $f(x, E)$ . Following Landau's approach,<sup>1</sup> we have first assumed that the dominant process is a two-quasiparticle interaction. Moreover the interaction is assumed to be local on the scale of variations of the distribution function. The kernel function  $K(\varepsilon)$  is proportional to the averaged squared interaction between two quasiparticles exchanging an energy  $\varepsilon$ . The scaling property observed for copper samples implies<sup>4</sup>  $K(\varepsilon) \propto \varepsilon^{-2}$ , as opposed to the AA prediction  $K(\varepsilon) \propto \varepsilon^{-3/2}$  for a diffusive conductor in the 1D regime.<sup>3</sup> In silver samples we have assumed that the interaction kernel still obeys a power law  $K(\varepsilon) = \kappa_\alpha \varepsilon^{-\alpha}$ , with  $\kappa_\alpha$  and  $\alpha$  taken as fitting parameters. These best fit theory curves, obtained with the parameters given in the columns "fit  $\kappa_\alpha \varepsilon^{-\alpha}$ " of Table 1, are plotted in Fig. 4 with full squares. For comparison, the best fits obtained with the exponent set at its predicted value  $\alpha = 3/2$  are plotted with open diamonds. Note that the same fitting parameters were used for all the samples

sample	parameters		fit $\kappa_\alpha \varepsilon^{-\alpha}$			fit TLS+AA		theory $\kappa_{3/2}^{\text{thy}}$
	w	D	$\alpha$	$\kappa_\alpha$	$\kappa_{3/2}$	$\kappa_{\text{TLS}}$	$\kappa_{3/2}$	
A5	90	0.011	$1.6 \pm 0.2$	1.02	1.30	$0.7 \pm 0.7$	$1.15 \pm 0.15$	0.14
B5,10	65	0.015	$1.4 \pm 0.2$	0.73	0.62	$0.9 \pm 0.9$	$0.41 \pm 0.21$	0.17
C20	160	0.023	$1.2 \pm 0.15$	1.23	0.70	$2.1 \pm 0.5$	$0.19 \pm 0.11$	0.06
D20a,b	100	0.020	$1.2 \pm 0.15$	0.95	0.49	$1.5 \pm 0.4$	$0.20 \pm 0.08$	0.10

Table 1. Samples parameters and fit parameters. The wire width  $w$  is in nm, the diffusion constant  $D$  in  $\text{m}^2\text{s}^{-1}$ . The fit parameters  $\kappa_\alpha$  are given in  $\text{ns}^{-1}\text{meV}^{\alpha-2}$ , and  $\kappa_{\text{TLS}}$  is given in  $\text{ns}^{-1}\text{meV}^{-1}$ .

of a given experiment. We obtained the exponent values  $\alpha = 1.6 \pm 0.2$  and  $1.4 \pm 0.2$  for experiments A and B, respectively, which are compatible with the prediction  $\alpha = 3/2$  (the diamonds in the top panels of Fig. 4 are practically superimposed with the squares). This compatibility is not found for the experiments C and D, for which  $\alpha = 1.2 \pm 0.15$ : the quality of the fits is visibly degraded by imposing  $\alpha = 3/2$ , as shown in the bottom panels of Fig. 4. The slope of the intermediate plateau in the theoretical curve (open diamonds) is systematically too large at  $U = 100 \mu\text{V}$  and  $U = 200 \mu\text{V}$ .

In order to explain the discrepancy between the predicted exponent  $\alpha = 3/2$  and the value  $\alpha = 1.2 \pm 0.15$  extracted from experiments C and D, we have investigated theoretically the effect of two-level systems (TLS) on the energy exchange between quasiparticles. The relevance of TLS on phase relaxation has recently been suggested by several authors.<sup>15,16</sup> We assume here that the quasiparticles are weakly coupled to the TLS, which are equally distributed along the wire. These TLS could be atoms moving across crystalline defects, or impurities in the crystal, for example. The TLS are assumed to have a flat energy distribution, and to be all equally coupled to the quasiparticles. We treat the absorption and emission of energy by the two-level systems in the perturbative limit: the absorption rate  $\Gamma_+^x(\varepsilon)$  (respectively the emission rate  $\Gamma_-^x(\varepsilon)$ ) by a TLS at position  $x$  with an energy separation  $\varepsilon$  is given by Fermi's golden rule:  $\Gamma_+^x(\varepsilon) = \lambda p_-^x(\varepsilon) h^x(\varepsilon)$  (resp.  $\Gamma_-^x(\varepsilon) = \lambda p_+^x(\varepsilon) h^x(-\varepsilon)$ ). In these expressions,  $\lambda$  is the coupling constant between quasiparticles and the TLS,  $p_-^x(\varepsilon)$  (resp.  $p_+^x(\varepsilon)$ ) is the occupation probability of the low-energy level (resp. the high-energy level), and  $h^x(\varepsilon) = \int dE f_E^x(1 - f_{E-\varepsilon})$ . Assuming that the TLS reach a local equilibrium with the quasiparticles, *i.e.*  $\Gamma_+^x(\varepsilon) = \Gamma_-^x(\varepsilon)$ , one obtains  $p_\pm^x(\varepsilon) = h^x(\pm\varepsilon)/(h^x(-\varepsilon) + h^x(\varepsilon))$ . Each term  $\lambda p_-(\varepsilon) f_E(1 - f_{E-\varepsilon})$  in  $\Gamma_+(\varepsilon)$  corresponds to an energy transfer of  $\varepsilon$  from a quasiparticle at energy  $E$  to a TLS. Therefore, it gives an “out” collision term in the Boltzmann equation

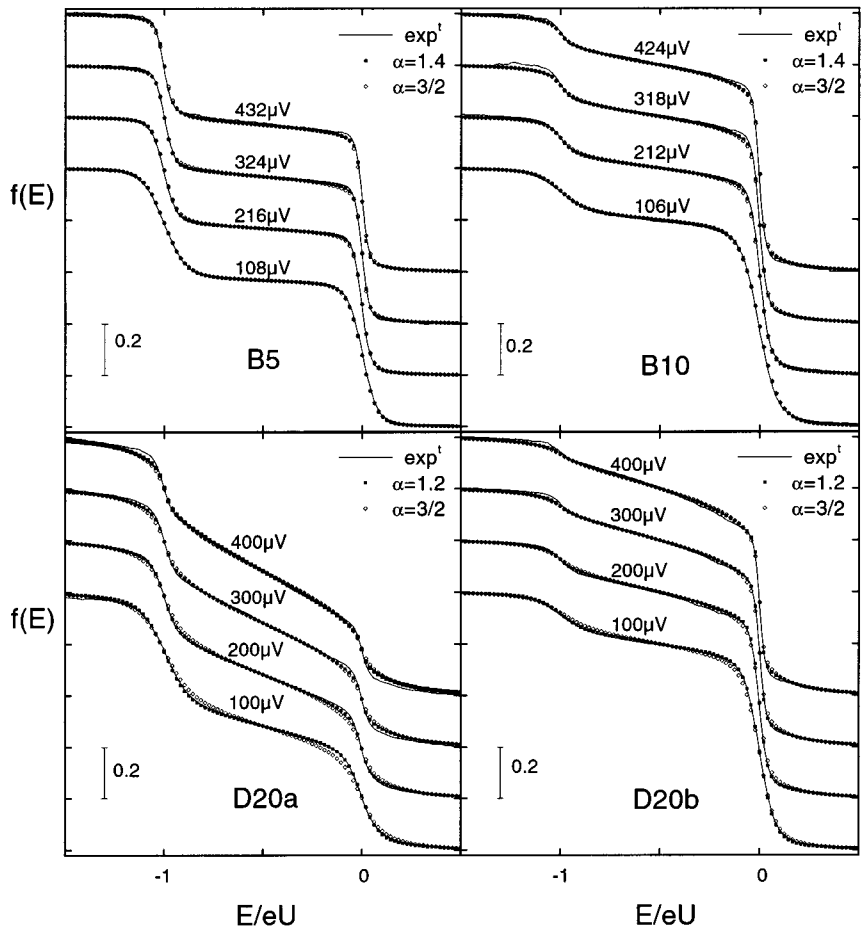


Fig. 4. Continuous lines in all four panels: measured distribution functions, plotted as a function of the reduced variable  $E/eU$  for  $U = 0.1, 0.2, 0.3$  and  $0.4$  mV, for the same samples as in Fig. 2. Successive curves were shifted vertically by 0.2, for clarity. Full squares are the best fits of the data to the solution of the Boltzmann equation with an interaction kernel  $K(\varepsilon) = \kappa_\alpha \varepsilon^{-\alpha}$ . Open diamonds are the best fits obtained with  $\alpha$  set to the theoretical value  $3/2$ , and adjusting the prefactor  $\kappa_{3/2}$ . Detailed fit parameters are given in Table 1.

(Eq. (1)) for quasiparticles at energy  $E$ . One then finds directly that the coupling to TLS can be written as an effective kernel function in Eq. (4), which depends on the local distribution function:  $K_{\text{eff}}^x(\varepsilon) = \kappa_{\text{TLS}}/(h^x(-\varepsilon) + h^x(\varepsilon))$ . The parameter  $\kappa_{\text{TLS}}$  is proportional to the density of TLS and to the coupling constant  $\lambda$ . The effective kernel  $K_{\text{eff}}^x(\varepsilon)$  is not a power-law function of  $\varepsilon$ : at energies large compared to  $eU$ ,  $K_{\text{eff}}^x(\varepsilon) \propto \varepsilon^{-1}$ , but  $K_{\text{eff}}^x(0)$  remains finite. Without assuming an unrealistic heating of the reservoirs, it was not possible to fit the data with this model alone. However, we found that all the experimental data could be well accounted for by assuming the presence of two phenomena: direct quasiparticle-quasiparticle interaction, described by the AA theory:<sup>3</sup>  $K(\varepsilon) = \kappa_{3/2}\varepsilon^{-3/2}$ ; and quasiparticle-TLS coupling, described by  $K_{\text{eff}}^x(\varepsilon)$ . The parameters  $\kappa_{\text{TLS}}$  and  $\kappa_{3/2}$  for the best fits (which are not shown because they are hardly distinguishable from the fits with the best value of  $\alpha$  in Fig. 4) are given in the columns “fits TLS+AA” of Table 1. Note that the error bars on  $\kappa_{\text{TLS}}$  and  $\kappa_{3/2}$  are correlated: the weighted sum of  $\kappa_{\text{TLS}}$  and  $\kappa_{3/2}$  must remain constant. Apart from sample A5, the theoretical value for  $\kappa_{3/2}^{\text{thy}}$  are of the same order of magnitude as  $\kappa_{3/2}$ . For the experiments A and B, extra contributions to AA theory are minimal. In contrast, in the experiments C and D the slope of the plateau in the distribution function is well explained by the TLS, whereas the AA mechanism, which dominates at low energy, is responsible for the rounding of the steps.

The differences that we observed between copper, gold and silver wires in the energy exchange rate experiments were also found in measurements of the phase coherence time  $\tau_\phi$  in wires fabricated using the same procedure. In a silver sample, the temperature dependence of  $\tau_\phi$  follows closely the theoretical prediction down to the base temperature  $T = 50$  mK of the refrigerator (where  $\tau_\phi = 9$  ns), whereas  $\tau_\phi$  saturates below 1 K at  $\tau_\phi = 1$  ns in our copper sample, and below 6 K at  $\tau_\phi = 10$  ps in our gold sample. These measurements are further discussed in this volume<sup>17</sup>.

In conclusion, we have found that interactions between quasiparticles in silver wires are much weaker and have a different qualitative behavior than in copper or gold wires. The energy exchange rate in our silver samples is close to the theoretical predictions for a diffusive medium in the 1D regime, provided that one includes an extra contribution, which might be due to two-level systems. The difference in the behavior of interactions in gold, copper and silver samples, as seen from the energy exchange rate experiments, is correlated to the measured saturation of  $\tau_\phi$  at low temperature which did occur in copper and gold, but not in silver. A possible interpretation could be that two-level systems are more numerous and/or better coupled to quasiparticles in copper and gold than in silver, leading to faster phase and energy relaxation. Moreover, preliminary calculations in the strong coupling regime

account for the scaling property of the distribution functions found in copper and gold samples.<sup>16</sup> Experiments are in progress to test this interpretation.

Acknowledgments: We are grateful to Norman Birge, P. Joyez, H. Kroha and C. Urbina for useful discussions and comments, and to P.F. Orfila for technical assistance. We acknowledge A. Steinbach for carefully reading the manuscript. This work has been partly founded by the Bureau National de la Métrologie.

## REFERENCES

1. D. Pines and P. Nozières, *The Theory of Quantum Liquids*, W.A. Benjamin (1966).
2. A. Schmid, *Z. Phys.* **271**, 251 (1974).
3. For a review, see B.L. Altshuler and A.G. Aronov, in *Electron-Electron Interactions in Disordered Systems*, Ed. A.L. Efros and M. Pollak, Elsevier Science Publishers B.V. (1985).
4. H. Pothier, S. Guéron, Norman O. Birge, D. Esteve, and M. H. Devoret, *Z. Phys. B* **104**, 178 (1997); *Phys. Rev. Lett.* **79**, 3490 (1997).
5. F. Pierre, H. Pothier, D. Esteve, and M.H. Devoret, unpublished.
6. J. M. Rowell and D.C. Tsui, *Phys. Rev. B* **14**, 2456 (1976).
7. R. Landauer, *IBM J. Res. Develop.* **1**, 223 (1957); **32**, 306 (1988).
8. In all the experiments we have performed (on copper, gold and silver wires), the sheet resistance of the aluminum probe was of the order of  $1\ \Omega$ . The superconducting finger was therefore far from the transition to an insulator, which makes the interpretation of our results in copper presented by B.N. Narozhny, I.L. Aleiner and B.L. Altshuler in *Phys. Rev. B* **60**, 7213 (1999) doubtful. Moreover, the stronger rounding of the distribution functions measured in longer wires, which was systematically observed in experiments, is in strong contradiction with the conclusions of this model.
9. D. Vion, P.F. Orfila, P. Joyez, D. Esteve, and M. H. Devoret, *J. Appl. Phys.* **77**, 2519 (1995).
10. The best fit was obtained with a reservoir temperature of 80 mK.
11. K.E. Nagaev, *Phys. Lett. A* **169**, 103 (1992); *Phys. Rev. B* **52**, 4740 (1995).
12. The width of this 5- $\mu\text{m}$ -long copper wire was  $w = 95\ \text{nm}$ , and the diffusion constant  $D = 0.0065\ \text{m}^2\text{s}^{-1}$ .
13. V.I. Kozub and A. M. Rudin, *Phys. Rev. B* **52**, 7853 (1995).
14. We have used here a numerical prefactor which was deduced (along the lines of the Appendix in Ref. 17) from the corrected expression of the phase coherence time  $\tau_\phi$  given in: I.L. Aleiner, B.L. Altshuler, and M.E. Gershenson, *Waves Random Media* **9**, 201 (1999). This prefactor is larger by a factor  $\pi\sqrt{2}$  than the one deduced from the expression of the lifetime in Eq. (4.4) of Ref. 3.
15. Y. Imry, H. Fukuyama and P. Schwab, *Europhys. Lett.* **47**, 608 (1999).
16. A. Zawadowski, Jan von Delft, D. C. Ralph, *Phys. Rev. Lett.* **83**, 2632 (1999); Johann Kroha and A. Zawadowski, private communication.
17. A.B. Gougam, F. Pierre, H. Pothier, D. Esteve, and N.O. Birge, this volume.